Published in final edited form as:
Phys Med Biol. 2013 February 21; 58(4): 807–823. doi:10.1088/0031-9155/58/4/807.

Comparison of risk of radiogenic second cancer following photon and proton craniospinal irradiation for a pediatric medulloblastoma patient

Rui Zhang[1,2,*], **Rebecca M Howell**[1,2], **Annelise Giebeler**[1,2], **Phillip J Taddei**[1,2,3], **Anita Mahajan**[2], and **Wayne D Newhauser**[1,2,4,5,**]

[1]Graduate School of Biomedical Sciences, The University of Texas at Houston, Houston, TX, USA

[2]Department of Radiation Physics and Radiation Oncology, The University of Texas MD Anderson Cancer Center, Houston, TX, USA

[3]Department of Radiation Oncology, Faculty of Medicine, American University of Beirut, Beirut, Lebanon

[4]Louisiana State University, Medical Physics Program, Department of Physics and Astronomy, Baton Rouge, LA, USA

[5]Mary Bird Perkins Cancer Center, Baton Rouge, LA, USA

Abstract

Pediatric patients who received radiation therapy are at risk of developing side effects like radiogenic second cancer. We compared proton and photon therapies in terms of the predicted risk of second cancers for a 4-year-old medulloblastoma patient receiving craniospinal irradiation (CSI). Two CSI treatment plans with 23.4 Gy or Gy (RBE) prescribed dose were computed: a three-field 6-MV photon therapy plan and a four-field proton therapy plan. The primary doses for both plans were determined using a commercial treatment planning system. Stray radiation doses for proton therapy were determined from Monte Carlo simulations, and stray radiation doses for photon therapy were determined from measured data. Dose-risk models based on the Biological Effects of Ionization Radiation VII report were used to estimate risk of second cancer in eight tissues/organs. Baseline predictions of the relative risk for each organ were always less for proton CSI than for photon CSI at all attained ages. The total lifetime attributable risks of the incidence of second cancer considered after proton CSI and photon CSI were 7.7% and 92%, respectively, and the ratio of lifetime risk was 0.083. Uncertainty analysis revealed that the qualitative findings of this study were insensitive to any plausible changes of dose-risk models and mean radiation weighting factor for neutrons. Proton therapy confers lower predicted risk of second cancer than photon therapy for the pediatric medulloblastoma patient.

Keywords

Proton therapy; second cancer; medulloblastoma; craniospinal irradiation; comparative treatment planning

**Corresponding author: Wayne D. Newhauser, Ph.D., Tel: 225-578-2262; newhauser@lsu.edu.
*Current address: Mary Bird Perkins Cancer Center, Baton Rouge, LA, USA

Conflict of Interest: none

1. Introduction

Medulloblastoma is one of the most common pediatric tumors of the central nervous system. The current standard of care includes surgery and a combination of craniospinal irradiation (CSI) and chemotherapy (Freeman *et al.*, 2002; Gottardo and Gajjar, 2006; Packer *et al.*, 2006; Packer and Vezina, 2008). The long-term survival rate for these patients has improved steadily over the past decades (Miralbell *et al.*, 2002; St Clair *et al.*, 2004; Fossati *et al.*, 2009), a change attributed primarily to postoperative radiation therapy (del Charco *et al.*, 1998). Typically, megavoltage external beam photon therapy (conventional radiotherapy) is used to treat the entire craniospinal axis. With conventional photon radiation, however, normal tissues outside the target receive a substantial radiation dose. Radiogenic late toxicities are of major concern in treating children because they may diminish lifespan and quality of life and can be physically and psychologically devastating to patients that survive their first cancer. Radiogenic late effects may occur months, years, or even decades after irradiation and may include second cancer, cardiac toxicity, pneumonitis, thyroiditis, cognitive deficiency, reduction in fertility and bone growth abnormalities. (Choux *et al.*, 1983; Hoppe-Hirsch *et al.*, 1990; Kiltie *et al.*, 1997; Mulhern *et al.*, 1998; Fossati *et al.*, 2009).

Avoiding potentially fatal complications, such as radiogenic second cancer, are of particular importance for pediatric patients because of their relatively longer survival time after their treatment and higher degree of radiation sensitivity compared to adults (Inskip and Curtis, 2007). Given that there is a latency period for development of a radiogenic second cancer, it is not possible to study the late effects of a contemporary radiation treatment technique before that technique becomes obsolete (NCRP, 2011). Alternatively, predictive risk models if available could be used to estimate pediatric patients' risk for developing radiation-induced late effects from contemporary treatment modalities (NCRP, 2011).

Until recently, there was limited knowledge involving accurate stray organ doses associated with technologically advanced contemporary radiation therapy. Calculation of dose from stray radiation is computationally complex, expensive, and has only recently become available for proton therapy (Jiang *et al.*, 2005; Zacharatou Jarlskog and Paganetti, 2008; Zhang *et al.*, 2008; Fontenot *et al.*, 2009; Newhauser *et al.*, 2009; Taddei *et al.*, 2009; Yepes *et al.*, 2010). Moreover, even if stray doses from advanced forms of radiation therapy are accurately computed, there remain several challenges to using risk models from the literature to predict late effects on the basis of organ doses. For example, most of the current dose-risk coefficients assume a linear non-threshold (LNT) model based on atomic bomb survivors data and are therefore intended for use with low dose (≤ 2.5 Sv) exposures. At higher doses, the cell sterilization mechanism may suppress risk because sterilized cells cannot, by definition, reproduce. Various dose-risk curves, such as the linear-exponential model and linear-plateau model, have been proposed in previous studies (Brenner *et al.*, 2000; Schneider *et al.*, 2005; Sigurdson *et al.*, 2005; Ronckers *et al.*, 2006b; Schneider *et al.*, 2008; Fontenot *et al.*, 2009; Rechner *et al.*, 2012). Furthermore, comparative risk assessments may vary substantially with the anatomical treatment site and other treatment- and host-specific factors, and with the methodology used for dose reconstruction and risk prediction. For those reasons, the literature on comparative risks of radiogenic late effects is incomplete, and there is a vital need for multidisciplinary inquiry into dose reconstruction and risk assessment (Newhauser, 2010).

St Clair *et al* (2004) reported a treatment planning comparison between three-dimensional conformal photon, intensity-modulated photon therapy and proton therapy for a pediatric patient with medulloblastoma. They found that proton therapy provided substantial greater sparing of normal-tissue than photon therapy and they opined that the long-term toxicity

such as cardiac dysfunction could be reduced by the dose sparing. Similar treatment planning studies (Miralbell *et al.*, 1997a; Miralbell *et al.*, 1997b; Lin *et al.*, 2000; Tarbell *et al.*, 2000; Lee *et al.*, 2005; Cochran *et al.*, 2008; Howell *et al.*, 2012) subsequently confirmed that proton therapy provides superior sparing of normal tissues compared to other techniques. Miralbell *et al* (2002) calculated the risk of second cancer after photon and proton radiation therapies for a 3-year-old boy with medulloblastoma and concluded that proton therapy can substantially reduce the second cancer risk. However, that study only considered spinal radiation treatment fields and did not include cranial treatment fields. In addition, the doses reported by Mirabell *et al* (2002) study were entirely based on treatment planning system (TPS) calculations that did not include stray radiation for proton therapy and underestimated stray radiation for photon therapy. Mu *et al* (2005) investigated different spinal irradiation techniques, and they recommended intensity modulated proton therapy (IMPT) for medulloblastoma patients instead of conventional photon therapy, intensity modulated photon radiation therapy (IMRT) or intensity modulated electron therapy. Again, they did not take stray radiation doses into account. Newhauser *et al* (2009) expanded upon the work of Miralbell *et al* (2002) by supplementing the therapeutic proton therapy doses with stray doses and calculating the predicted incidence of second cancer after CSI. They reported that proton therapies carried a substantially lower predicted risk than photon therapies. However, Newhauser *et al* [17] did not account for the underestimation of stray doses reported by the TPS for photon therapy. Brodin *et al* (Brodin *et al.*, 2011) recently estimated risks of radiation-induced adverse late effects, including second cancer, in pediatric medulloblastoma patients following proton and photon CSI. They concluded that the intensity-modulated proton therapy compared favorably to the photon techniques in terms of all radiobiological risk estimates. In their study, they used organ-specific neutron doses from Newhauser *et al* (2009).

In all these previous studies, the risks of late effects were either not calculated (St Clair *et al.*, 2004) or were calculated on the basis of age and sex non-specific risk coefficients from International Commission on Radiological Protection (ICRP) reports (Miralbell *et al.*, 2002; Mu *et al.*, 2005; Taddei *et al.*, 2009). These studies also had limited consideration of organ-specific equivalent doses from stray radiation. Stray radiation from proton therapy was either not included (Miralbell *et al.*, 2002; Mu *et al.*, 2005) or estimated within a small spherical receptor put in the organs of a computational phantom (Newhauser *et al.*, 2009; Brodin *et al.*, 2011). Similarly, stray radiation from photon therapy was underestimated by all of these studies (Miralbell *et al.*, 2002; Mu *et al.*, 2005; Taddei *et al.*, 2009; Brodin *et al.*, 2011) because commercial TPS systems significantly underestimate out-of-field dose (Howell *et al.*, 2010a). Thus the literature provides incomplete information on dose reconstructions particularly in regard to stray dose for both photon and proton CSI.

The aim of this work was to compare contemporary proton and photon therapies in terms of the risks of second cancers for a pediatric patient receiving CSI using clinically realistic and physically complete dose reconstructions. Both therapeutic and secondary radiation doses were included in the risk calculations. We determined primary doses from treatment plans which were calculated using a commercial TPS. We then determined secondary doses from Monte Carlo simulations for proton therapy and from TPS and measurements for photon therapy. The primary and stray components of organ dose were summed and used in combination with risk models in the literature to predict the risk of developing radiogenic second cancers from proton and photon CSI. Finally, we evaluated the robustness of the qualitative findings through rigorous uncertainty analysis.

2. Methods and materials

2.1 Patient and treatment planning

A 4-year-old boy diagnosed with medulloblastoma was chosen for this study to facilitate comparison with previous studies from Miralbell *et al* (2002) and Newhauser *et al* (2009) both of which considered a 3-year old boy. The patient was treated in the supine position with proton CSI in our clinic at MD Anderson Cancer Center. Computed tomography (CT) images were obtained from the top of the head to the thigh. Both proton and photon treatment plans were created using a commercial TPS (Eclipse version 8.9, Varian Medical Systems, Palo Alto, CA), which was previously commissioned for clinical use (Newhauser *et al.*, 2007). All treatment plans were calculated using a 2.5-mm calculation grid with heterogeneity corrections. Both photon and proton treatment planning were carried out according to the standard of care at our institution. Details treatment plans are briefly described in the following paragraphs and a more thorough description can be found in the literature (Giebeler *et al.*, 2012; Howell *et al.*, 2012). The final plans for this patient were approved by one of us (A Mahajan), a board certified radiation oncologist who specializes in pediatric radiation oncology. To facilitate plan comparison, we adjusted the total prescribed dose to 23.4 Gy relative biological effectiveness (RBE) (i.e., 21.3 Gy × 1.1 to reflect the biological effectiveness of protons relative to photons) and 23.4 Gy for the proton and photon CSI treatment plans, respectively. Posterior fossa boost fields were not considered in this study. However, this is not expected to have a substantial effect on the second cancer risk predictions for either photon or proton therapy. In an earlier study Taddei *et al* (2009) reported that the contribution from stray dose from the boost fields in proton CSI was negligible to the organs considered here, i.e., far from the treatment field. Similarly, for photon therapy stray dose is low at large distances from the field, especially for a small field (like those used for boost fields) (Stovall *et al.*, 1995). Furthermore, the prescribed dose from the boost fields was substantially less than for the primary fields.

For proton treatment, the passively scattered proton beam line at MD Anderson Cancer Center Proton Therapy Center (Arjomandy *et al.*, 2009) was used. We used an age-specific target volume for this patient according to the standard of practice at our institution for proton CSI (Giebeler *et al.*, 2012). Because this patient was younger than 15 years of age, the target volume included the cranial and spinal cavities, the meninges, as well as the entirety of the vertebral bodies (in older patients, the vertebral body is not included). This larger target volume is believed to reduce the risk of asymmetric growth of the vertebral body for younger patients whose spines are still maturing (St Clair *et al.*, 2004; Brodin *et al.*, 2011). The proton treatment plan included right and left posterior oblique cranial fields and two posterior-anterior spinal fields. Patient-specific devices included a range compensator and field-defining collimator. The characteristics of the proton therapy beams for this patient are listed in table 1. Proton treatments at our institution include one to three junction shifts, to reduce dosimetric heterogeneities at the field junctions. However, For this study, we did not include junction shifts in the final proton plan because the dosimetric heterogeneities at the field junctions do not extend beyond the target and therefore do not extend into the organs at risk for second cancer. The plan was initially calculated with junction shifts and then the junction shifts were removed and the plan was reoptimized to achieve approximately the same uniformity as the plan with shifts.

The photon treatment plan included two opposed-lateral cranial fields (gantry angles of 270° and 90°) and one posterior-anterior spinal field (gantry angle of 180°) that encompassed the length of spinal axis. All photon fields were 6 MV. The target volume included cranial and spinal cavities. The final photon plan included junction shifts after 9 Gy and 16.2 Gy. Because dosimetric heterogeneities at the junctions of photon beams extend beyond the target depth and into organs at risk for developing a second cancer, the junction shifts for the

photon plans could not be neglected and organ doses were based on a sum plan that included junction shifts. An intensity-modulated field-in-field (FIF) technique was used to reduce dose heterogeneity within the cranial and spinal fields (Yom *et al.*, 2007).The FIF technique uses multiple lower-weighted reduction fields, which contained blocked segments strategically placed within primary cranial and spinal fields to reduce the highest dose areas and to force greater homogeneity in the target volume. Additional details about the photon CSI treatment planning methods were reported by Howell *et al* (2012).

The organs of interest for radiogenic cancer include the stomach, colon, lungs, bladder, thyroid, liver, prostate and remainder (*i.e.,* all other tissues/organs for which organ-specific risk coefficients were not explicitly provided in the Biological Effects of Ionizing Radiation [BEIR] VII report (NRC, 2006)). These organs were delineated on the planning CT images for each patient. Radiogenic skin cancer and leukemia were excluded in this study because the CT image data set did not extend inferiorly to include skin and bone marrow in their entireties.

Therapeutic and stray dose reconstructions—The therapeutic organ doses from proton and photon therapies were both taken from the dose-volume histograms (DVH) calculated by the TPS. The stray dose in proton therapy was calculated by Monte Carlo simulations using Monte Carlo code (MCNPX version 2.6, Los Alamos National Laboratory, Los Alamos, NM; (Hendricks *et al.*, 2006)) because its suitability for simulating doses in proton therapy has been well established. The treatment plan was imported into an in-house Monte Carlo Proton Radiotherapy Treatment Planning (MCPRTP) system (Newhauser *et al.*, 2007; Newhauser *et al.*, 2008) which utilizes the MCNPX code and a detailed model of the beamline. Because stray neutrons originated from both the treatment unit (external neutrons) and the patient (internal neutrons), separate simulations were performed to estimate dose from external and internal neutrons. The total neutron dose was obtained by summation. Details of the simulation tools have been described in previous studies (Newhauser *et al.*, 2007; Newhauser *et al.*, 2009; Taddei *et al.*, 2009).

Because stray dose from photon therapy is underestimated by the commercial TPS, additional data were needed to account for this. In a previous study, Howell *et al.* (2010a) reported that the absorbed dose values for 6 MV photons reported by this TPS were accurate above the 5% isodose level. In a subsequent study, Howell *et al* (2010b), described a method to report organ dose for in-field, partially in-field, and out-of-field organs based on where the organ is positioned with respect to the 5% isodose line. Using that method, we determined organ doses from the photon treatment plan by the following three criteria (1) if an organ was entirely within the 5% isodose, dose was assumed to be accurately reported by the TPS; (2) if an organ was entirely outside of the 5% isodose, dose was estimated using thermoluminescent dosimeter (TLD) measurements in an anthropomorphic phantom; and (3) if the organ was partially within the 5% isodose, dose was determined using the TPS and measured data with a volume-weighting approach.

A CT scan of the anthropomorphic phantom (ATOM, CIRS, Inc., Norfork, VA) was acquired and then imported into the TPS. A 6 MV FIF photon treatment plan was developed to irradiate the entire cranial and spinal regions of the phantom. The treatment plan was consistent with the patient treatment planning methodology already described. Measurement locations were defined throughout the phantom at various distances from the field edge. Lithium fluoride TLD-100 powder capsules (Quantaflux Radiological Services, San Jose, CA) were loaded into the phantom, which was irradiated by a clinical linear accelerator (Clinac 2100, Varian Medical Systems, Palo Alto, Ca) with the planned treatment fields. Following irradiation, the TLDs were individually read using an established laboratory protocol from the Accredited Dosimetry Calibration Laboratory at MD Anderson Cancer

Center. A calibration coefficient was used to convert TLD readings to absorbed dose in tissue.

The equivalent dose, H_T, in each organ, T, was calculated by multiplying the organ absorbed dose, D_T, by the mean radiation weight factor, $\overline{w_R}$. The $\overline{w_R}$ value was taken as 1.1 for proton beams (an average quality factor for therapeutic proton beams) and 1 for photon beams. For stray neutrons, $\overline{w_R}$ values were taken from a study by Newhauser *et al* (2009) that simulated neutron spectral fluence within the organs of an anthropomorphic phantom receiving CSI, and they calculated $\overline{w_R}$ values based on recommendations from ICRP Publication 92 (2003). Their mean $\overline{w_R}$ values were 7.75 for the cranial field, 8.09 for the superior spinal field and 8.17 for the inferior spinal field. These values were applied to the corresponding fields in this study, and the average of the superior and inferior spinal field $\overline{w_R}$ values was used for middle spinal field in this study.

Calculation of risk of second cancers—The models described in the BEIR VII report (NRC, 2006) were used to calculate risk of radiogenic second cancer on the basis of radiation doses in radiosensitive organs and tissues. The risk of developing a radiogenic cancer depends on many host and treatment factors, including the amount of radiation, age at exposure, attained age, and sex. Allowing for adjustments of the models based on these factors, the BEIR-VII report provided organ-specific linear non-threshold (LNT) risk models suitable for the estimation of excess relative risk (*ERR*) at low-dose and low-dose rate exposures. For each organ or tissue, T, ERR_T was defined as:

$$ERR_T = RR_T - 1, \quad (1)$$

where RR_T is relative risk for the organ or tissue T and was defined as the ratio of disease incidence rates in exposed groups to that of unexposed groups.

For any given organ or tissue the BEIR-VII report recommended the following formula to calculate ERR_T:

$$ERR_T = \beta_s H_T \exp(\gamma e^*)\left(\frac{a}{60}\right)^{\eta}, \quad (2)$$

where H_T is the equivalent dose in Sv and is the sum of doses from therapeutic fields and stray radiation doses generated from each therapeutic field to a certain organ, e is age at exposure in years, e^* is $(e - 30)/10$ for $e < 30$ and zero for $e > 30$, and a is attained age in years, β_s is the sex-specific and organ-specific instantaneous *ERR*/Sv value, γ is the per-decade increase in age at exposure over the interval 0–30 years, and η is the exponent of attained age. Values for β_s, γ, and η were taken for a boy from Table 12-2 of BEIR VII for each organ and tissue. Using these data and equation (2), we estimated risks of second cancers at various attained ages, *e.g.*, at 15, 30, 45, 60, 75 and 95 years after radiotherapy. For each organ, we defined Ratio of Relative Risk (*RRR*) as

$$RRR = RR_h / RR_p, \quad (3)$$

where the subscript h denotes proton therapy, and subscript p denotes photon therapy.

The BEIR VII report defined Excess Absolute Risk (*EAR*) as the difference between the cancer incidence rates of the exposed and unexposed groups. The report also defined lifetime attributable risk (*LAR*) as the probability that an irradiated patient will develop a radiation-induced cancer during his or her lifetime (at attained age 100 years) exposed to certain equivalent dose H_T at age e, and it recommended that *LAR* should be estimated

using both relative and absolute risk transport models. The *LAR* coefficients of cancer incidence were provided in table 12D-1 in the BEIR VII report, and we used the values for a 4-year-old boy to calculate cumulative lifetime risk of second cancer incidence. The risk coefficients in table 12D-1 included a dose and dose-rate reduction factor (DDREF) of 1.5, which only applies to low dose (<100 mGy) and low dose rate (<0.01 mGy/min). The DDREF was thus taken out by us in the following *LAR* risk calculations. For simplicity, *EAR* coefficients from the BEIR VII report were used to calculate the cumulative risk of radiogenic second cancer incidence of this patient living to certain years to compare with Childhood Cancer Survivor Study (CCSS) data (see discussion section). Because probabilities of surviving to those attained ages conditional on survival to age at exposure (Arias, 2010) were very close to unity, they were not taken into account in cumulative risk calculations.

For each modality, the *LAR* was calculated as

$$LAR_{modality}=\left(\sum_{T} LAR_T\right)_{modality}, \quad (4)$$

where the sum is over all the organs or tissues. To compare the risks of proton versus photon therapies, the Ratio of Lifetime Attributable Risk (*RLAR*) was defined as

$$RLAR=LAR_h/LAR_p. \quad (5)$$

again the subscript *h*, *p* denotes proton therapy and photon therapy, respectively.

Uncertainty—Risk calculations are subject to a variety of uncertainties, which could affect the predicted late effects. Rigorous uncertainty analysis is necessary to ensure that baseline risk estimates are robust to such uncertainties. This section describes the uncertainty analysis used to investigate the effects of deviations from the baseline assumptions. Specifically, we considered uncertainty in the type of dose response model and uncertainty in the mean radiation weighting factor for neutrons.

Fontenot *et al* (2010) estimated the uncertainties in risk calculations following photon and proton radiotherapies for prostate cancer on the basis of rigorous error propagation and sensitivity tests. The following equation was based on the formalism of Fontenot *et al* (2010) and was modified for *RLAR*:

$$\left(\frac{\sigma_{RLAR}}{RLAR}\right)^2=\left(\frac{\sum_T LAR_1^2\left(\frac{\sigma_{D_T^1}}{D_T^1}\right)^2+LAR_2^2\left(\frac{\sigma_{D_T^2}}{D_T^2}\right)^2}{\left(\sum_T LAR_T\right)^2}\right)_h+\left(\frac{\sum_T LAR_1^2\left(\frac{\sigma_{D_T^1}}{D_T^1}\right)^2+LAR_2^2\left(\frac{\sigma_{D_T^2}}{D_T^2}\right)^2}{\left(\sum_T LAR_T\right)^2}\right)_p \quad (6)$$

where $\left(\frac{\sigma_{RLAR}}{RLAR}\right)$ is the relative uncertainty in *RLAR*, $\left(\frac{\sigma_{D_T^1}}{D_T^1}\right)$ is the relative uncertainty in the therapeutic dose, and $\left(\frac{\sigma_{D_T^2}}{D_T^2}\right)$ is the relative uncertainty in the stray dose.

The baseline calculations of second cancer risk utilized the LNT model, which is mostly based on low dose data (<2.5 Sv) from atomic bomb survivors (NRC, 2006). At higher

doses, the cell sterilization mechanism may be important (Sigurdson *et al.*, 2005; Ronckers *et al.*, 2006a; Bhatti *et al.*, 2010) and other possible dose-response relationships, *e.g.* linear-plateau relation and linear-exponential relationship, may better reflect response to radiation therapy doses (Hall and Wuu, 2003; Schneider and Kaser-Hotz, 2005). The uncertainty analysis of the dose-response model was applied to the calculated risk of second cancer in thyroid because of the strong evidence that the dose-risk relationship for thyroid is not linear (Sigurdson *et al.*, 2005; Ronckers *et al.*, 2006a; Bhatti *et al.*, 2010). For the sensitivity test, the LNT model, linear-exponential models and linear-plateau models with different inflection points (figure 3) were used. Because the highest equivalent dose to thyroid in the proton plan was less than 0.4 Sv and the LNT model is valid for the dose range 0~2.5 Sv, the different dose-risk models were tested only for the photon plan, where higher exit doses make cell sterilization relevant.

There are large uncertainties in neutron RBE values for carcinogenesis (Newhauser *et al.*, 2009; Fontenot *et al.*, 2010). A sensitivity test was carried out by recalculating the risk for various neutron weighting factors, from $\overline{w_R}/2$ to $\overline{w_R} \times 25$, based on Kellerer *et al* (2006).

RESULTS

Figure 1(a) and (b) show proton and photon therapeutic absorbed dose distributions for this 4-year-old boy. The dose fall-off in the photon plan is much more gradual than that for the proton plan, resulting in higher doses in regions anterior to the vertebral bodies. This was true even with the larger target volume used in the proton plan which included the vertebral bodies in addition to the cranial and spinal cavities. Figure 1(c) shows the stray neutron dose distribution from proton CSI. Although the stray neutron dose is much lower in magnitude than the therapeutic proton dose, it penetrates the whole body of the patient and is not negligible. Figure 2 plots DVHs for therapeutic radiation doses from photon and proton CSI plans. From this figure, it is apparent that while both plans provided good coverage of their respective target volumes (described in Methods), the proton plan resulted in superior sparing of normal tissue for every organ considered in this study.

Table 2 lists mean organ equivalent doses from proton and photon CSI treatment plans for this patient. Total equivalent doses are listed for both photon and proton CSI. For proton CSI, therapeutic and stray doses are both provided because these data were available directly from the Monte Carlo simulations. For photon CSI, only the total equivalent dose values are listed because it is not possible to delineate components of stray photon dose based on phantom measurements or TPS calculations. The equivalent dose to the remainder, which includes any organ for which risk coefficients were not explicitly provided in the BEIR VII report, was estimated as the mean dose of the other organs listed in table 2. For each organ and for the remainder, the equivalent dose was at least a factor of 4 higher for photon therapy than for proton therapy. The smallest ratios (i.e., largest factor differences) were found in the thyroid, bladder, and colon.

The baseline values of relative risk at various time intervals after exposure (15, 30, 45, 60, 75, and 95 years) are listed in table 3. At 15 years after exposure, the highest *RR* values for proton therapy were for stomach cancer, colon cancer and other solid tumors and the highest values for photon therapy were for thyroid cancer, colon cancer, and other solid tumors. In contrast, at 95 years after exposure, the highest *RR* value for proton therapy was for thyroid cancer while for photon therapy the highest values were for thyroid cancer, colon cancer, and liver cancer. The *RR* values decreased with increasing time after exposure for all solid cancers except thyroid cancer.

Table 3 also lists the predicted *RRR* values for each cancer site and various years after exposure. The calculated *RRR* values were much less than 1 at 15, 30, 45 and 60 years after exposure. Notably, the *RRR* values increased with increasing time after exposure for all cancers except thyroid cancer. All predicted baseline *RRR* values were less than 1, indicating a lower predicted risk following proton CSI than following photon CSI for all radiogenic second cancers.

The *LAR* following proton CSI was predicted at 11.6%, that following photon CSI was 138%, and the *RLAR* was 0.083 (95% confidence interval is 0.081–0.085). The reason that *LAR* following photon CSI was higher than 100% can be explained as that this patient may develop multiple second cancers in his lifetime, which has been revealed by CCSS data (Armstrong *et al.*, 2011). The relationship between predicted *RLAR* and maximum weighting factor for neutrons is shown in figure 4. As the mean radiation weighting factor for neutrons increased, the *LAR* values for proton therapy increased because the H_T values increased for stray neutrons, resulting in the final *RLAR* values increasing with increasing neutron radiation weighting factor. Only after the maximum weighting factor for neutrons exceeded 20 times that of the values recommended by the ICRP (2003) (i.e., maximum w_R value greater than 400) was the *RLAR* greater than 1.

Table 4 lists the predicted *RR* and *RRR* values for each of the thyroid dose-risk models studied. The *RR* values in photon CSI showed substantial sensitivity to the selected risk model. Dose-risk models with the low dose roll-off points markedly suppressed the predicted risk from high doses, thus reducing the *RR* value from photon CSI, while increasing the *RRR* value since the *RR* value from proton CSI was not changed. However, the predicted *RRR* values were still less than 1, ranging from 0.055 to 0.36.

4. Discussion

Radiation doses and second cancer risks were calculated for both photon and proton CSI in a 4-year-old boy, taking into account clinically realistic and physically complete reconstruction of primary and stray radiation exposures. We found that proton CSI conferred a lower predicted risk of radiogenic second cancer than photon CSI for all cancer types and times after exposure that were considered in this study.

The uncertainty analysis demonstrated that the *RLAR* values were sensitive to the mean radiation weighting factor $\overline{w_R}$ for neutrons, and the *RRR* value for thyroid cancer was sensitive to whether cell sterilization was accounted for in the dose-risk model. However, for plausible values of $\overline{w_R}$ and considering all scenarios of cell sterilization effects, the qualitative findings of the study were insensitive to uncertainties in $\overline{w_R}$ values and the existence or magnitude of plausible cell sterilization effects.

Our results agree well with those of previous studies. Newhauser *et al* (2009) reported predicted lifetime risks of second cancer incidence for a 3-year-old boy at 5.1% for passively-scattered proton therapy and 54.8% for conventional photon therapy following 36 Gy CSI. If normalized to the same prescribed dose, the lifetime second cancer incidences in our work are higher than those in their work (Table 5). That study used different dose reconstruction methods and risk prediction models than ours and these are the major reasons for the moderate differences in predicted cancer incidence. Specifically, the risk coefficients from BEIR VII for the patient we studied (a 4-year-old boy) are generally higher than those from ICRP Publication 60, since a young patient is more prone to develop radiogenic second cancers than the general population. If we roughly adjusted the risk values from Newhauser *et al* by age (multiplying the risk coefficient from ICRP Publication 60 by the ratio between the risk coefficients for a 4-year-old boy and coefficients for a 30-year-old man in BEIR

VII), their lifetime risks of second cancer incidence would be 106% and 9.5% after photon and proton CSI, which are much closer to the corresponding risk values reported here. Therefore, after we adjusted the dose-risk coefficient values by age and sex so that the risk models were similar, our values were similar values to those of Newhauser *et al* (2009).

Our results agree well with those of Newhauser *et al* (2009) regarding the ratio of predicted lifetime risk for second cancer incidence after photon and proton CSI. Specifically, they reported a ratio of 11, while we report a ratio of 12. Given the differences in methods used for risk calculations, as already discussed, the ratio of risk values are remarkably similar. One possible reason is that, although different methods were used in the two studies, using the ratio of risk values as a figure of merit cancels some sources of uncertainty, such as uncertainties associated with risk models and dose reconstruction methods. This finding underscores the pivotal importance of the use of the ratio of risks as a robust figure of merit for research comparing treatment modalities.

Our stray radiation doses for proton therapy agree well with those from Taddei *et al* (2010) who estimated lifetime risk of second cancer incidence and mortality for a boy and a girl due to stray neutron dose from proton CSI with 23.4 Gy (RBE) prescription. Their predicted risk value for a 10-year-old boy was 8.5% lifetime attributable incidence. Bone marrow and skin were included in their calculation, while our work did not take those two tissues into account. After subtracting second cancer risks from those two tissues, their lifetime risk value for the boy was 5.5%, which agrees very well with our lifetime risk value of 4.6% due to stray neutrons. Their risk value was slightly higher than ours, even for an older patient, because they used a smaller air gap between the patient and final beam defining collimator was used in the spinal fields in their study. Their smaller air gap (2 cm) resulted in higher external neutron doses than if the air gap had been 12 cm air gap used in our study.

Brodin *et al* (2011) compared risks of second cancer and other late effects for 10 pediatric medulloblastoma patients following photon and proton CSI. They estimated average lifetime risks to be 45% and 7% for three-dimensional conformal photon therapy (3D CRT) and intensity-modulated proton therapy (IMPT), respectively, using the organ equivalent dose (OED) concept and the linear-plateau model (Schneider and Walsh, 2008). It is difficult to directly compare our results with theirs because we used a different initial slope of the dose-response curves, and Brodin *et al* did not report their organ doses, nor are their organ-specific model parameters available. However, the qualitative findings of the two studies are consistent in that both studies concluded that proton therapy will greatly reduce the risk of radiogenic second cancer, even with secondary neutron dose included.

It is interesting to compare our predicted risk calculations with the CCSS epidemiological second cancer incidence data (Meadows *et al.*, 2009). The cumulative incidence of second malignant neoplasms in childhood cancer survivors based on follow-up data was around 2% and 9% at 15 years and 30 years since diagnosis. We compared their values to cumulative *EAR* values in our study for corresponding time after exposure. In our study, the cumulative *EAR* values for photon CSI were 0.5% and 4.4% at 15 years and 30 years time since exposure, respectively; and 0.05% and 0.5% for proton CSI at 15 years and 30 years time since exposure. A possible explanation for the higher incidence in the epidemiological data is that it included second cancers from radiation and other causes, such as chemotherapy, possible genetic predispositions, and unrecognized environmental factors, In contrast, our result was based on second cancer risk from radiation only.

Our study has several strengths. First, we used realistic patient data from clinically deployed TPS and the risk calculations were based on the dose distributions from clinically realistic CSI treatment fields. Second, the advanced dose reconstruction tools we used provided us

with both therapeutic and stray radiation doses for photon and proton CSI, enabling us to prepare the most accurate and comprehensive evaluation of radiation doses and risks for CSI patients that has been achieved. Third, rigorous uncertainty analysis reinforced our qualitative findings.

This study had some limitations. First, because of time and resource limitations, only one pediatric patient was used for radiogenic second cancer risk estimation. Calculations based on more patients may give us additional information and provide a better comparison between different modalities. This work is currently underway in our laboratory. Second, dose measurements at selected positions within the phantom were used to estimate mean organ stray dose in photon therapy, while Monte Carlo simulations were used to determine stray dose in proton therapy. This could introduce systematic uncertainties to the comparison of dose and risk between these two modalities. However, to our knowledge, those TLD measurement data are the most accurate and up-to-date stray radiation data for photon CSI. In light of the results from this and previous investigations, it appears that these limitations are minor in the context of the objectives of this work.

5. Conclusion

Proton CSI carried a significantly lower predicted risk of radiogenic second cancer than photon CSI in a pediatric patient. Sensitivity analysis revealed that quantitative values were sensitive to uncertainties in the risk model and the mean radiation weighting factor for neutrons. However, the qualitative findings of the study were insensitive to any plausible changes of dose-risk models and $\overline{w_R}$ values. Similar studies should be carried out for girls and boys of other ages at exposure and for other advanced radiation treatment modalities, such as helical tomotherapy and volumetric modulated arc therapy (VMAT).

Acknowledgments

The authors are grateful to Kathryn Carnes for their assistance in preparing and editing this manuscript. This work was supported by Sowell-Huggins Scholarship (RZ), President Research Scholarship (RZ), the National Cancer Institute (award 1R01CA131463-01A1) (WDN), Northern Illinois University through a subcontract of a Department of Defense contract (award W81XWH-08-1-0205) (WDN) and the National Institutes of Health Fogarty International Center (award K01TW008409) (PJT).

References

Arias E. United States life tables, 2006. National vital statistics reports : from the Centers for Disease Control and Prevention, National Center for Health Statistics, National Vital Statistics System. 2010; 58:1–40.

Arjomandy B, Sahoo N, Zhu XR, Zullo JR, Wu RY, Zhu M, Ding X, Martin C, Ciangaru G, Gillin MT. An overview of the comprehensive proton therapy machine quality assurance procedures implemented at The University of Texas M. D. Anderson Cancer Center Proton Therapy Center-Houston. Med Phys. 2009; 36:2269–82. [PubMed: 19610316]

Armstrong GT, Liu W, Leisenring W, Yasui Y, Hammond S, Bhatia S, Neglia JP, Stovall M, Srivastava D, Robison LL. Occurrence of multiple subsequent neoplasms in long-term survivors of childhood cancer: a report from the childhood cancer survivor study. J Clin Oncol. 2011; 29:3056–64. [PubMed: 21709189]

Bhatti P, Veiga LH, Ronckers CM, Sigurdson AJ, Stovall M, Smith SA, Weathers R, Leisenring W, Mertens AC, Hammond S, Friedman DL, Neglia JP, Meadows AT, Donaldson SS, Sklar CA, Robison LL, Inskip PD. Risk of second primary thyroid cancer after radiotherapy for a childhood cancer in a large cohort study: an update from the childhood cancer survivor study. Radiat Res. 2010; 174:741–52. [PubMed: 21128798]

Brenner DJ, Curtis RE, Hall EJ, Ron E. Second malignancies in prostate carcinoma patients after radiotherapy compared with surgery. Cancer. 2000; 88:398–406. [PubMed: 10640974]

Brodin NP, Rosenschold PM, Aznar MC, Kiil-Berthelsen A, Vogelius IR, Nilsson P, Lannering B, Bjork-Eriksson T. Radiobiological risk estimates of adverse events and secondary cancer for proton and photon radiation therapy of pediatric medulloblastoma. Acta Oncol. 2011; 50:806–16. [PubMed: 21767178]

Choux M, Lena G, Hassoun J. Prognosis and long-term follow-up in patients with medulloblastoma. Clin Neurosurg. 1983; 30:246–77. [PubMed: 6667578]

Cochran DM, Yock TI, Adams JA, Tarbell NJ. Radiation dose to the lens during craniospinal irradiation-an improvement in proton radiotherapy technique. Int J Radiat Oncol Biol Phys. 2008; 70:1336–42. [PubMed: 18029111]

del Charco JO, Bolek TW, McCollough WM, Maria BL, Kedar A, Braylan RC, Mickle JP, Buatti JM, Mendenhall NP, Marcus RB Jr. Medulloblastoma: time-dose relationship based on a 30-year review. Int J Radiat Oncol Biol Phys. 1998; 42:147–54. [PubMed: 9747832]

Fontenot JD, Bloch C, Followill D, Titt U, Newhauser WD. Estimate of the uncertainties in the relative risk of secondary malignant neoplasms following proton therapy and intensity-modulated photon therapy. Phys Med Biol. 2010; 55:6987–98. [PubMed: 21076196]

Fontenot JD, Lee AK, Newhauser WD. Risk of secondary malignant neoplasms from proton therapy and intensity-modulated x-ray therapy for early-stage prostate cancer. Int J Radiat Oncol Biol Phys. 2009; 74:616–22. [PubMed: 19427561]

Fossati P, Ricardi U, Orecchia R. Pediatric medulloblastoma: toxicity of current treatment and potential role of protontherapy. Cancer Treat Rev. 2009; 35:79–96. [PubMed: 18976866]

Freeman CR, Taylor RE, Kortmann RD, Carrie C. Radiotherapy for medulloblastoma in children: a perspective on current international clinical research efforts. Med Pediatr Oncol. 2002; 39:99–108. [PubMed: 12116057]

Giebeler A, Howell R, Amos R, Mahajan A, Newhauser W. Standardized treatment planning methodology for passively scattered proton craniospinal irradiation and consistency between individually optimized plans. Medical Dosimetry. 2012 (in review).

Gottardo NG, Gajjar A. Current therapy for medulloblastoma. Curr Treat Options Neurol. 2006; 8:319–34. [PubMed: 16942675]

Hall EJ, Wuu CS. Radiation-induced second cancers: the impact of 3D-CRT and IMRT. Int J Radiat Oncol Biol Phys. 2003; 56:83–8. [PubMed: 12694826]

Hendricks, JS.; McKinney, GW.; Durkee, JW.; Finch, JP.; Fensin, ML.; James, MR.; Johns, RC.; Pelowitz, DB.; Waters, LS.; Gallmeier, FX. MCNPX, Version 26c. Los Alamos National Laboratory; 2006.

Hoppe-Hirsch E, Renier D, Lellouch-Tubiana A, Sainte-Rose C, Pierre-Kahn A, Hirsch JF. Medulloblastoma in childhood: progressive intellectual deterioration. Childs Nerv Syst. 1990; 6:60–5. [PubMed: 2340529]

Howell R, Giebeler A, Koontz-Raisig W, Mahajan A, Etzel C, D'Amelio A Jr, Homann KWN. Comparison of therapeutic dosimetric data from passively scattered proton and photon craniospinal irradiations for medulloblastoma. Radiation Oncology. 2012 (in review).

Howell RM, Scarboro SB, Kry SF, Yaldo DZ. Accuracy of out-of-field dose calculations by a commercial treatment planning system. Phys Med Biol. 2010a; 55:6999–7008. [PubMed: 21076191]

Howell RM, Scarboro SB, Taddei PJ, Krishnan S, Kry SF, Newhauser WD. Methodology for determining doses to in-field, out-of-field and partially in-field organs for late effects studies in photon radiotherapy. Phys Med Biol. 2010b; 55:7009–23. [PubMed: 21076193]

ICRP. Ann ICRP. Oxford: International Commission on Radiological Protection; 2003. Relative biological effectiveness (RBE), quality factor (Q), and radiation weighting factor (w_R). Publication 92; p. 1-117.

Inskip PD, Curtis RE. New malignancies following childhood cancer in the United States, 1973–2002. Int J Cancer. 2007; 121:2233–40. [PubMed: 17557301]

Jiang H, Wang B, Xu XG, Suit HD, Paganetti H. Simulation of organ-specific patient effective dose due to secondary neutrons in proton radiation treatment. Phys Med Biol. 2005; 50:4337–53. [PubMed: 16148397]

Kellerer AM, Ruhm W, Walsh L. Indications of the neutron effect contribution in the solid cancer data of the A-bomb survivors. Health Phys. 2006; 90:554–64. [PubMed: 16691103]

Kiltie AE, Lashford LS, Gattamaneni HR. Survival and late effects in medulloblastoma patients treated with craniospinal irradiation under three years old. Med Pediatr Oncol. 1997; 28:348–54. [PubMed: 9121399]

Lee CT, Bilton SD, Famiglietti RM, Riley BA, Mahajan A, Chang EL, Maor MH, Woo SY, Cox JD, Smith AR. Treatment planning with protons for pediatric retinoblastoma, medulloblastoma, and pelvic sarcoma: how do protons compare with other conformal techniques? Int J Radiat Oncol Biol Phys. 2005; 63:362–72. [PubMed: 16168831]

Lin R, Hug EB, Schaefer RA, Miller DW, Slater JM, Slater JD. Conformal proton radiation therapy of the posterior fossa: a study comparing protons with three-dimensional planned photons in limiting dose to auditory structures. Int J Radiat Oncol Biol Phys. 2000; 48:1219–26. [PubMed: 11072181]

Meadows AT, Friedman DL, Neglia JP, Mertens AC, Donaldson SS, Stovall M, Hammond S, Yasui Y, Inskip PD. Second neoplasms in survivors of childhood cancer: findings from the Childhood Cancer Survivor Study cohort. J Clin Oncol. 2009; 27:2356–62. [PubMed: 19255307]

Miralbell R, Lomax A, Bortfeld T, Rouzaud M, Carrie C. Potential role of proton therapy in the treatment of pediatric medulloblastoma/primitive neuroectodermal tumors: reduction of the supratentorial target volume. Int J Radiat Oncol Biol Phys. 1997a; 38:477–84. [PubMed: 9231669]

Miralbell R, Lomax A, Cella L, Schneider U. Potential reduction of the incidence of radiation-induced second cancers by using proton beams in the treatment of pediatric tumors. Int J Radiat Oncol Biol Phys. 2002; 54:824–9. [PubMed: 12377335]

Miralbell R, Lomax A, Russo M. Potential role of proton therapy in the treatment of pediatric medulloblastoma/primitive neuro-ectodermal tumors: spinal theca irradiation. Int J Radiat Oncol Biol Phys. 1997b; 38:805–11. [PubMed: 9240650]

Mu X, Bjoerk-Eriksson T, Nill S, Oelfke U, Johansson K-A, Gagliardi G, Johansson L, Karlsson M, Zackrisson DB. Does electron and proton therapy reduce the risk of radiation induced cancer after spinal irradiation for childhood medulloblastoma? A comparative treatment planning study. Acta Oncologica. 2005; 44:554–62. [PubMed: 16165914]

Mulhern RK, Kepner JL, Thomas PR, Armstrong FD, Friedman HS, Kun LE. Neuropsychologic functioning of survivors of childhood medulloblastoma randomized to receive conventional or reduced-dose craniospinal irradiation: a Pediatric Oncology Group study. J Clin Oncol. 1998; 16:1723–8. [PubMed: 9586884]

NCRP. Second Primary Cancers and Cardiovascular Disease After Radiation Therapy. Bethesda, MD: 2011.

Newhauser W. Complexity of advanced radiation therapy necessitates multidisciplinary inquiry into dose reconstruction and risk assessment. Phys Med Biol. 2010; 55

Newhauser W, Fontenot J, Zheng Y, Polf J, Titt U, Koch N, Zhang X, Mohan R. Monte Carlo simulations for configuring and testing an analytical proton dose-calculation algorithm. Phys Med Biol. 2007; 52:4569–84. [PubMed: 17634651]

Newhauser WD, Fontenot JD, Mahajan A, Kornguth D, Stovall M, Zheng Y, Taddei PJ, Mirkovic D, Mohan R, Cox JD, Woo S. The risk of developing a second cancer after receiving craniospinal proton irradiation. Phys Med Biol. 2009; 54:2277–91. [PubMed: 19305036]

Newhauser WD, Zheng Y, Taddei PJ, Mirkovic D, Fontenot JD, Giebeler A, Zhang R, Titt U, Mohan R. Monte Carlo proton radiation therapy planning calculations. Trans Am Nucl Soc. 2008:2.

NRC. Health Risks from Exposure to Low Levels of Ionizing Radation: BEIR VII - Phase 2. Washington, D.C: Nation Research Council of the National Academies; 2006.

Packer RJ, Gajjar A, Vezina G, Rorke-Adams L, Burger PC, Robertson PL, Bayer L, LaFond D, Donahue BR, Marymont MH, Muraszko K, Langston J, Sposto R. Phase III study of craniospinal radiation therapy followed by adjuvant chemotherapy for newly diagnosed average-risk medulloblastoma. J Clin Oncol. 2006; 24:4202–8. [PubMed: 16943538]

Packer RJ, Vezina G. Management of and prognosis with medulloblastoma: therapy at a crossroads. Arch Neurol. 2008; 65:1419–24. [PubMed: 19001159]

Rechner LA, Howell RM, Zhang R, Etzel C, Lee AK, Newhauser WD. Risk of radiogenic second cancers following volumetric modulated arc therapy and proton arc therapy for prostate cancer. Phys Med Biol. 2012; 57:7117–32. [PubMed: 23051714]

Ronckers CM, Sigurdson AJ, Stovall M, Smith SA, Mertens AC, Liu Y, Hammond S, Land CE, Neglia JP, Donaldson SS, Meadows AT, Sklar CA, Robison LL, Inskip PD. Thyroid cancer in childhood cancer survivors: a detailed evaluation of radiation dose response and its modifiers. Radiat Res. 2006a; 166:618–28. [PubMed: 17007558]

Ronckers ET, Groot W, Steenbakkers M, Ruland E, Ament A. Costs of the 'Hartslag Limburg' community heart health intervention. BMC Public Health. 2006b; 6:51. [PubMed: 16512909]

Schneider U, Kaser-Hotz B. A simple dose-response relationship for modeling secondary cancer incidence after radiotherapy. Z Med Phys. 2005; 15:31–7. [PubMed: 15830782]

Schneider U, Lomax A, Timmermann B. Second cancers in children treated with modern radiotherapy techniques. Radiother Oncol. 2008; 89:135–40. [PubMed: 18707783]

Schneider U, Walsh L. Cancer risk estimates from the combined Japanese A-bomb and Hodgkin cohorts for doses relevant to radiotherapy. Radiat Environ Biophys. 2008; 47:253–63. [PubMed: 18157543]

Schneider U, Zwahlen D, Ross D, Kaser-Hotz B. Estimation of radiation-induced cancer from three-dimensional dose distributions: Concept of organ equivalent dose. Int J Radiat Oncol Biol Phys. 2005; 61:1510–5. [PubMed: 15817357]

Sigurdson AJ, Ronckers CM, Mertens AC, Stovall M, Smith SA, Liu Y, Berkow RL, Hammond S, Neglia JP, Meadows AT, Sklar CA, Robison LL, Inskip PD. Primary thyroid cancer after a first tumour in childhood (the Childhood Cancer Survivor Study): a nested case-control study. Lancet. 2005; 365:2014–23. [PubMed: 15950715]

St Clair WH, Adams JA, Bues M, Fullerton BC, La Shell S, Kooy HM, Loeffler JS, Tarbell NJ. Advantage of protons compared to conventional X-ray or IMRT in the treatment of a pediatric patient with medulloblastoma. Int J Radiat Oncol Biol Phys. 2004; 58:727–34. [PubMed: 14967427]

Stovall M, Blackwell CR, Cundiff J, Novack DH, Palta JR, Wagner LK, Webster EW, Shalek RJ. Fetal dose from radiotherapy with photon beams: report of AAPM Radiation Therapy Committee Task Group No. 36. Med Phys. 1995; 22:63–82. [PubMed: 7715571]

Taddei PJ, Mirkovic D, Fontenot JD, Giebeler A, Zheng Y, Kornguth D, Mohan R, Newhauser WD. Stray radiation dose and second cancer risk for a pediatric patient receiving craniospinal irradiation with proton beams. Phys Med Biol. 2009; 54:2259–75. [PubMed: 19305045]

Tarbell NJ, Smith AR, Adams J, Loeffler JS. The challenge of conformal radiotherapy in the curative treatment of medulloblastoma. Int J Radiat Oncol Biol Phys. 2000; 46:265–6. [PubMed: 10661330]

Yepes PP, Mirkovic D, Taddei PJ. A GPU implementation of a track-repeating algorithm for proton radiotherapy dose calculations. Phys Med Biol. 2010; 55:7107–20. [PubMed: 21076192]

Yom SS, Frija EK, Mahajan A, Chang E, Klein K, Shiu A, Ohrt J, Woo S. Field-in-field technique with intrafractionally modulated junction shifts for craniospinal irradiation. Int J Radiat Oncol Biol Phys. 2007; 69:1193–8. [PubMed: 17967308]

Zacharatou Jarlskog C, Paganetti H. Risk of developing second cancer from neutron dose in proton therapy as function of field characteristics, organ, and patient age. Int J Radiat Oncol Biol Phys. 2008; 72:228–35. [PubMed: 18571337]

Zhang G, Liu Q, Zeng S, Luo Q. Organ dose calculations by Monte Carlo modeling of the updated VCH adult male phantom against idealized external proton exposure. Phys Med Biol. 2008; 53:3697–722. [PubMed: 18574316]

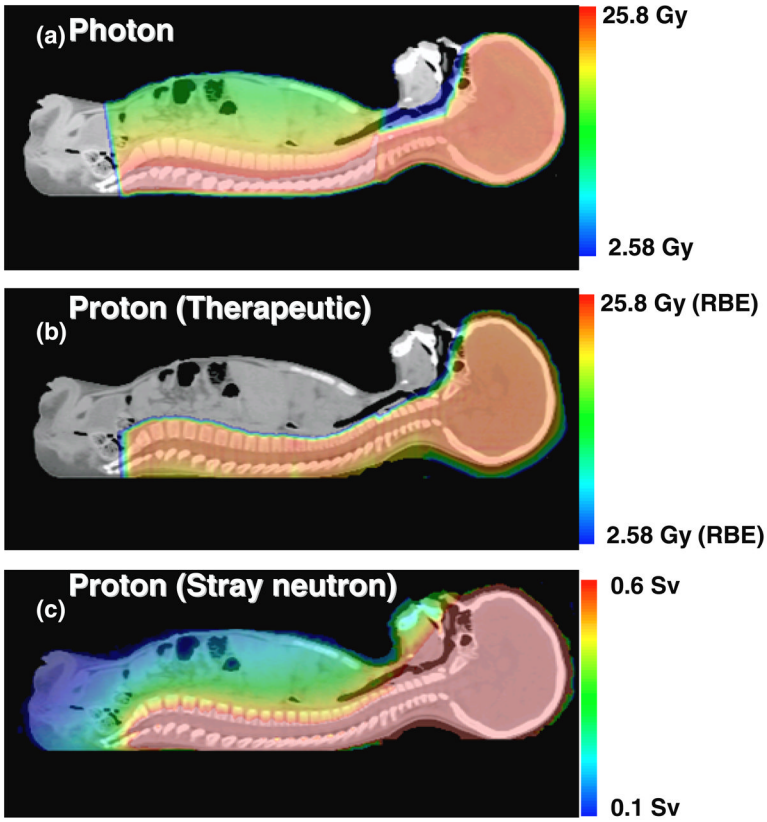

Figure 1.
Dose distributions for a 4-year-old boy receiving photon CSI (a) or proton CSI (b), and the stray neutron dose distribution (c) generated during proton CSI.

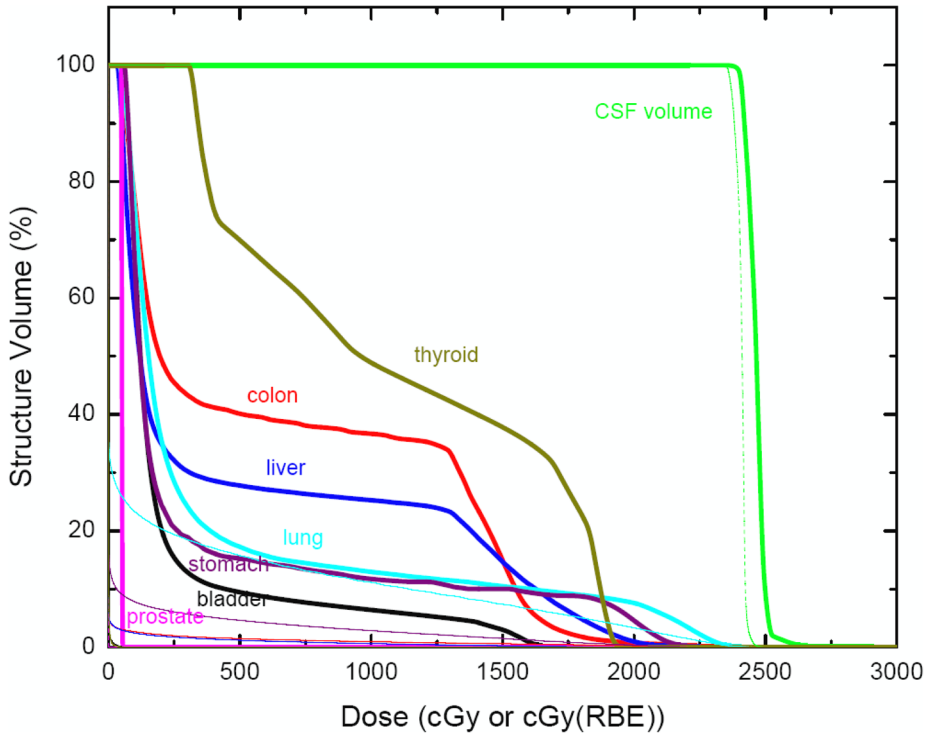

Figure 2.
Dose-volume histograms from the treatment plans (thick line for photon, thin line for proton) for various organs. Proton doses for some organs are less than 1 Gy and are difficult to visualize on this figure.

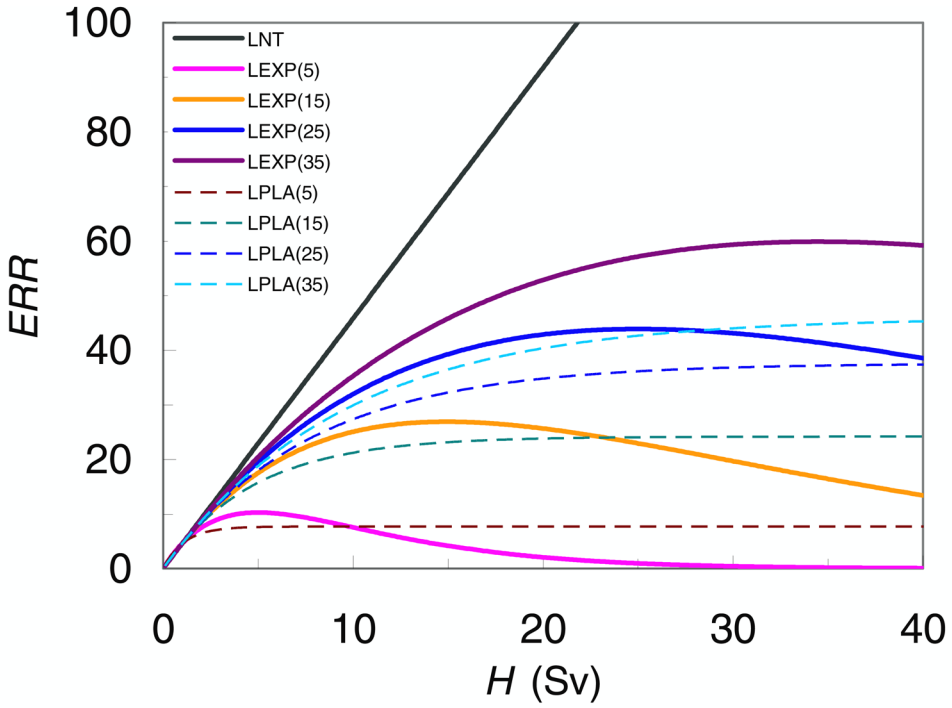

Figure 3.

Excess relative risk (*ERR*) as a function of equivalent dose, *H*. LEXP (linear-exponential) and LPLA (linear-plateau) models were used in this work to estimate *ERR* in the thyroid. The numbers in the legend refer to the location of the approximate dose point beyond which *ERR* decreases or plateaus. The different dose-risk models were tested only for the photon plan considering very low dose to thyroid in the proton plan.

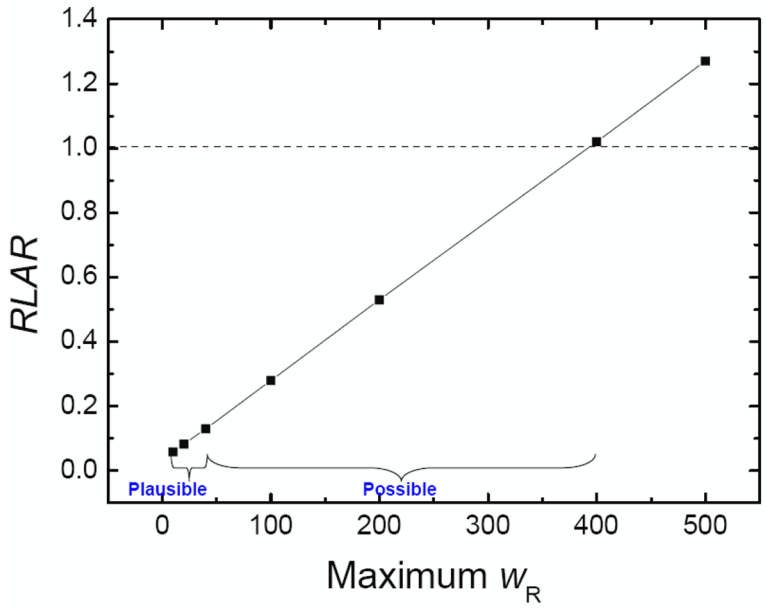

Figure 4.

Sensitivity of the ratio of lifetime attributable risk (*RLAR*) values to changes in the maximum radiation weighting factor for neutrons. The plausible interval extends from 8 to 40 (NRC, 2006). However, an analysis by Kellerer *et al* (2006) suggested the interval could possibly extend up to 400.

Table 1

Selected proton beam parameters of the CSI fields.

Parameters	Cranium	Cranium	Upper spine	Lower spine
Proton energy at nozzle entrance (MeV)	180	180	160	160
Range in patient (cm H_2O)	16	15.7	10.9	10.7
SOBP width (cm H_2O)	16	16	5	6
Gantry angle (degree)	255	105	180	180
Air gap (cm)	10.8	11.3	11.5	11.8
Aperture thickness (cm)	6	6	4	4
Proximal margin around CTV (cm)	0.3	0.3	0.3	0.4
Distal margin around CTV (cm)	0.8	0.8	−0.2	0
Ratio of field size to brass aperture size	0.6	0.6	0.34	0.38

SOBP denotes spread-out break peak; CTV denotes clinical target volume.

Table 2

Mean organ dose (without radiation weighting factor) and organ equivalent doses from proton and photon CSI plans for a 4-year-old boy. For proton CSI, therapeutic, stray and total doses are listed. For photon CSI, the combined doses from both therapeutic and stray doses are listed. (Because of the methodology used to calculate photon dose, it was not possible to separate therapeutic dose from stray dose for photon CSI).

Organ	D_h (mGy)		H_h (mSv)			D_p (mGy) Total	H_p (mSv) Total	$H_{h,\text{total}}/H_{p,\text{total}}$
	Therapeutic	Stray	Therapeutic	Stray	Total			
Prostate	1	20	1	159	160	1662	1662	0.096
Colon	150	26	165	209	374	6415	6415	0.058
Lungs	225	41	248	329	577	4413	4413	0.131
Stomach	612	36	673	289	962	4076	4076	0.236
Bladder	5	21	5	170	175	3127	3127	0.056
Liver	155	31	171	249	420	5493	5493	0.076
Thyroid	5	48	6	383	389	10854	10854	0.036
Remainder	165	32	181	255	437	5149	5149	0.085

Subscript *h* denotes proton therapy, and subscript *p* denotes photon therapy.

Table 3

Baseline calculations of relative risk of radiogenic second cancer for a 4-year-old boy. Relative risk for each organ (RR_T) is shown, and the corresponding ratio of relative risk ($RRR = RR_{T,h}/RR_{T,p}$) following photon and proton CSI at 15, 30, 45, 60, 75 and 95 years after treatment.

	15 years			30 years			45 years			60 years			75 years			95 years		
Organs	$RR_{T,h}$	$RR_{T,p}$	RRR	$RR_{T,h}$	$RR_{T,p}$	RRR	$RR_{T,h}$	$RR_{T,p}$	RRR	$RR_{T,h}$	$RR_{T,p}$	RRR	$RR_{T,h}$	$RR_{T,p}$	RRR	$RR_{T,h}$	$RR_{T,p}$	RRR
Stomach	3.204	10.340	0.310	1.976	5.136	0.385	1.585	3.479	0.456	1.403	2.706	0.518	1.300	2.270	0.573	1.219	1.926	0.633
Colon	3.571	45.101	0.079	2.138	20.527	0.104	1.682	12.706	0.132	1.470	9.055	0.162	1.350	6.998	0.193	1.255	5.373	0.234
Liver	2.467	20.181	0.122	1.649	9.493	0.174	1.389	6.092	0.228	1.268	4.503	0.282	1.199	3.609	0.332	1.145	2.902	0.395
Lung	3.015	16.410	0.184	1.892	7.823	0.242	1.535	5.090	0.302	1.368	3.814	0.359	1.274	3.096	0.412	1.200	2.528	0.475
Prostate	1.210	3.176	0.381	1.093	1.964	0.557	1.056	1.578	0.669	1.038	1.397	0.743	1.028	1.296	0.794	1.021	1.216	0.840
Bladder	1.955	18.061	0.108	1.423	8.554	0.166	1.253	5.529	0.227	1.174	4.116	0.285	1.130	3.320	0.340	1.095	2.692	0.407
Thyroid	2.784	50.782	0.055	2.784	50.782	0.055	2.784	50.782	0.055	2.784	50.782	0.055	2.784	50.782	0.055	2.784	50.782	0.055
Other	7.440	76.878	0.096	2.263	15.876	0.142	1.454	6.347	0.229	1.215	3.531	0.344	1.119	2.404	0.466	1.063	1.746	0.609

Subscript *h* denotes proton therapy, and subscript *p* denotes photon therapy.

Table 4

Predicted *RR* and *RRR* values in thyroid for various dose-risk models plotted in figure 3 for the nominal $\overline{w_R}$ value. The dose-risk models include: linear non-threshold (LNT); linear-exponential (LEXP) and linear-plateau (LPLAT).

Dose-Risk Model	*RR*		*RRR*
	Proton (*H*=0.39 Sv)	Photon (*H*=10.85 Sv)	
LNT	2.78	50.81	0.055
LEXP (5)	2.78	7.65	0.36
LEXP (15)	2.78	22.79	0.12
LEXP (25)	2.78	30.89	0.09
LEXP (35)	2.78	35.24	0.079
LPLAT (5)	2.78	8.63	0.32
LPLAT (15)	2.78	20.31	0.14
LPLAT (25)	2.78	26.33	0.11
LPLAT (35)	2.78	29.10	0.096

The numbers in parentheses indicate the equivalent dose in Sv at which the risk rolls off because of the cell sterilization effect (i.e., the inflection point).

Table 5

Comparison of lifetime attributable risk of second cancer incidence and ratio of the lifetime risk after proton CSI versus photon CSI (23.4 Gy or Gy (RBE)) from three studies.

	Lifetime risk (%)		Ratio of lifetime risks (photon/proton)
	Photon	Proton	
Miralbell *et al* (2002)	35.6	2.4	15
Newhauser *et al* (2009)	35.6*	3.3	11
This work	138	11.6	12

* Data reproduced from Miralbell *et al* (2002).

Table 6

Comparison of stray organ equivalent doses after proton CSI from three studies.

Organs	H_T/D (mSv/Gy)		
	This work	**Taddei *et al* (2009)**	**Newhauser *et al* (2009)**
Prostate	6.8	4.5	0.8
Colon	8.9	15.4	4.7
Lungs	14.1	28.1	8.0
Stomach	12.4	19.8	5.9
Bladder	7.3	6.7	1.4
Liver	10.6	20.7	5.7
Thyroid	16.4	31.6	12.3
Remainder	10.9	16.1	4.8